Scilight

Low-Dimensional Materials
https://www.sciltp.com/journals/ldm

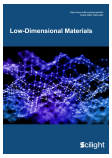

Review

Advances in Understanding the Mechanisms of Moiré Ferroelectricity

Yuanming Ye [1], Jiawei Li [1] and Yutong Ran [2,*]

[1] State Key Lab of New Ceramic Materials, School of Materials Science and Engineering, Tsinghua University, Beijing 100084, China
[2] Grikin Advanced Materials Co. Ltd., Beijing 102200, China
* Correspondence: ran_yutong@163.com

How To Cite: Ye, Y.; Li, J.; Ran, Y. Advances in Understanding the Mechanisms of Moiré Ferroelectricity. *Low-Dimensional Materials* **2026**, *2*(2), 5. https://doi.org/10.53941/ldm.2026.100005

Received: 7 May 2026
Revised: 15 June 2026
Accepted: 17 June 2026
Published: 26 June 2026

Abstract: Moiré ferroelectricity provides a platform for regulating interfacial polarization in two-dimensional van der Waals materials through local stacking, lattice reconstruction and mesoscale domain formation. In these systems, polarization is governed by interlayer symmetry breaking, charge redistribution, orbital hybridization, lattice relaxation, strain gradients and electronic screening. This review summarizes recent progress in graphene/hBN, twisted hBN, rhombohedral transition metal dichalcogenides and marginally twisted transition metal dichalcogenides, and discusses how these systems have advanced the understanding of moiré-scale polarization. This mechanistic understanding has evolved together with characterization methods, from electrical hysteresis and local electrostatic mapping to multimodal analysis of stacking structures, domain-wall dynamics and polarization vector fields. The review then analyzes polarization origins, including stacking-dependent interfacial dipoles, reconstructed polar domains, electrostatic imprinting and electronically assisted polarization. It also discusses polarization switching and domain-wall dynamics, emphasizing local stacking conversion, domain-wall migration, dislocation-network rearrangement, soliton-network evolution and pinning-depinning processes. Furthermore, it clarifies the distinction between ordinary periodic polar-domain patterns and topological polar textures, which require vector-field reconstruction, in-plane polarization rotation, winding or chirality, and structural correlation with domain walls or saddle-point regions. Finally, this review outlines perspectives on operando characterization under device-relevant conditions, ultrafast switching, multi-field control and deterministic domain-wall engineering.

Keywords: two-dimensional materials; moiré ferroelectricity; polarization mechanism; interfacial polarization; domain-wall dynamics; topological polar textures

1. Introduction

Ferroelectricity requires stable dipole order, reversible electric-field-driven switching and retention of the switched polar state [1]. However, scaling conventional three-dimensional ferroelectrics down to the few-unit-cell limit remains challenging because depolarization fields, incomplete charge screening and interface-driven structural relaxation can destabilize the polar phase [2–5]. The weak interlayer coupling, chemically saturated surfaces, and atomically sharp interfaces of two-dimensional (2D) van der Waals (vdW) materials help stabilize polar order at the atomic-thickness limit [2,6]. In these systems, switchable polarization can originate from either the non-centrosymmetric crystal lattice or the relative registry between adjacent layers [4,7]. The former is represented by intrinsic 2D ferroelectrics, such as metal phosphorus chalcogenides [8–10] and layered ferroelectric

semiconductors [11,12]. Sliding and interfacial ferroelectricity shift switchable polarization to a stacking- and interface-controlled property and expand the origin of ferroelectricity. Interfacial ferroelectricity refers to ferroelectric polarization generated at a non-centrosymmetric vdW interface [13]. This polarization originates from stacking-dependent charge redistribution, orbital hybridization and ionic relaxation across adjacent layers. Sliding ferroelectricity refers to a switching mechanism in which in-plane interlayer translation reverses the out-of-plane polarization [14,15]. In these systems, local stacking registry determines the polarization direction, and interlayer sliding connects stacking states with opposite polarization. Parallel-stacked hBN [13,16] and rhombohedral bilayer TMDs [14,17,18] are representative systems. In these systems, local stacking registry determines the polarization direction, and interlayer sliding connects stacking states with opposite polarization.

Moiré ferroelectricity refers to switchable polarization that is controlled by local stacking registry and organized by a moiré superlattice [16,19]. A small twist angle or lattice mismatch creates a long-period moiré superlattice, which periodically modulates local atomic alignment, interlayer coupling and the electrostatic environment [20–22]. This modulation reorganizes stacking-dependent interfacial dipoles into moiré-scale polar domains, charge-polarized interfacial superlattices or moiré-dependent ferroelectric responses [14,19,23]. Moiré ferroelectricity was first demonstrated in graphene-based moiré heterostructures and charge-polarized twisted hBN interfaces [16,19,23]. This mesoscopic moiré superlattice scale is a key advantage of moiré ferroelectricity. It links atomic-scale stacking rules to device-scale polar responses and has driven rapid progress in recent years. In these systems, twist angle, lattice mismatch and lattice reconstruction determine the spatial arrangement of polar domains and the resulting polar response [19,23–25]. Notably, spatially alternating dipoles or moiré electrostatic potentials can appear before reversible switching is established [26,27].

Theoretical studies established an early basis for linking local stacking to moiré-scale polarity. In 2017, Li and Wu used first-principles calculations to predict vertical ferroelectricity in binary-compound 2D bilayers and multilayers, showing that lateral interlayer translation reversed out-of-plane polarization and that small twist or strain could generate a ferroelectric moiré superlattice [28]. Later theoretical work extended this stacking-polarity picture across several levels. First-principles calculations linked local stacking registry to interlayer charge redistribution, out-of-plane dipole density, stacking energy and sliding barriers, and showed why AB/BA or MX/XM domains carry opposite polar states [27]. Continuum elasticity and lattice-relaxation models showed that interlayer adhesion competes with intralayer elastic cost and electrostatic energy, leading to reconstructed moiré-scale polar domains, finite-width domain walls and field-dependent changes in the area fraction of adjacent stacking domains [18,26]. Electrostatic screening models showed that dielectric response and mobile carriers modify gate-field coupling, local potential contrast and hysteretic switching, which is important for separating intrinsic polarization reversal from screening-related responses [29]. Vector-polarization and domain-wall models further predicted that domain walls and saddle-point regions can host in-plane polarization components, giving rise to domain-wall-mediated switching pathways and topological polar textures [30,31]. Together, these studies supplied a physical map that connects atomic stacking, lattice relaxation, electrostatic screening and domain-wall structure with the formation and motion of polar domains in moiré ferroelectrics.

Building on these theoretical insights, the understanding of moiré ferroelectricity has progressed from the recognition of moiré-scale polarization responses to the real-space resolution of polar domains, switching dynamics and topological polar textures, as shown in Figure 1. Early experiments demonstrated moiré-scale polarization responses in graphene-based moiré heterostructures, charge-polarized twisted hBN interfaces and marginally twisted TMD bilayers in 2020 and 2021, respectively [14,19,23]. These studies identified local stacking and interfacial charge redistribution as key contributors to polar states across moiré superlattices. They also left open how hysteresis, electrostatic contrast and domain patterns should be linked to specific microscopic mechanisms. Subsequent work moved from phenomenological identification to real-space and functional readout. Electrostatic mapping resolved moiré potentials in twisted hBN [32], plasmonic and nano-photocurrent measurements visualized ferroelectric domains in graphene/twisted-WSe_2 structures [33], and ferroelectric WTe_2/WSe_2 superlattices demonstrated switchable moiré potentials [24]. Remote moiré ferroelectricity further showed that polar superlattices can engineer the electronic structure of adjacent 2D materials [34]. More recent studies have advanced the field from static polar landscapes to dynamics and programmability. Operando electron microscopy revealed polar-domain dynamics in marginally twisted WSe_2 homobilayers [35]. Rotationally engineered WSe_2 trilayers further showed that interlayer twist sequences can tune the spatial ordering and switching dynamics of polar domains [36]. Mechanical force-induced sliding was further demonstrated in parallel-stacked hBN, showing that local force can drive interlayer displacement, dipole reversal and domain motion in interfacial ferroelectrics [37]. In parallel, vector-resolved and manipulation-based studies have begun to identify topological polar textures confined to moiré interfaces, marking a new stage in which moiré ferroelectricity is understood as a platform for programmable and topologically structured polar order [25,38].

These milestones also identify several coupled control parameters. For example, twist angle sets the moiré length scale and strongly affects polar-domain dynamics, as shown by operando electron microscopy in twisted bilayer WSe_2 [35]. Charge redistribution creates spatially varying moiré potentials, which can be detected directly in twisted hBN [32] or remotely imprinted from twisted WSe_2 onto graphene [34]. Lattice relaxation, strain and flexoelectricity reshape polar domains and domain walls in marginally twisted hBN [39]. Interlayer sliding provides a switching coordinate for dipole reversal and domain motion in engineered vdW multilayers and mechanically modulated interfacial ferroelectrics [36,37]. These observations have established multiple experimental signatures of moiré ferroelectricity, but their microscopic interpretation remains system-dependent. Electrostatic, optical, operando and mechanical probes are sensitive to different physical quantities. Because moiré superlattices couple local stacking, lattice relaxation, strain, electrostatics and switching dynamics, the microscopic mechanism of moiré ferroelectricity remained under discussion in the early stage of the field [29].

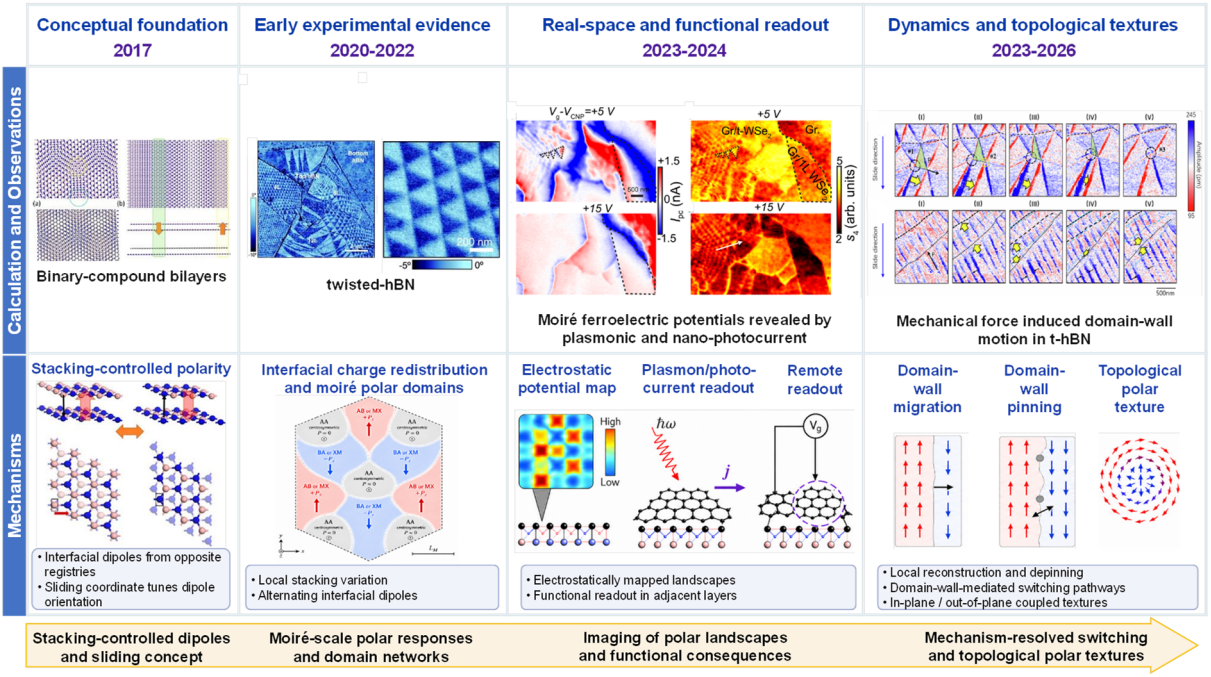

Figure 1. Milestones in the discovery and mechanistic understanding of moiré ferroelectricity. Adapted with permission from [28]. Copyright 2017 American Chemical Society. Copyright 2021, Springer Nature [23]. Copyright 2023, Springer Nature [33]. Copyright 2025, Springer Nature [37].

These debates highlight the need to resolve moiré ferroelectricity across structure, electrostatics and domain dynamics. Early polar responses could be interpreted in terms of stacking-dependent dipoles, interfacial charge redistribution, lattice reconstruction, strain coupling or domain-wall motion. Recent advances in electrostatic mapping, near-field optical imaging, nano-photocurrent measurements and operando microscopy have begun to clarify these contributions in real space. These methods now correlate polarization response with local atomic alignment, reconstruction and domain evolution. The characterization-driven progress provides the foundation for a mechanism-oriented review of moiré ferroelectricity. This review therefore examines how recent experimental and theoretical advances have deepened the understanding of polarization origin, switching behavior and emergent polar textures in moiré ferroelectricity. These unresolved questions also raised the evidentiary standard for the field. Individual signals such as hysteresis, electrostatic contrast, piezo-response or optical readout can indicate polar order, but they do not by themselves determine its microscopic origin or switching pathway. Mechanism-resolved understanding therefore requires correlated structural, electrostatic, electromechanical and operando evidence.

This review focuses on recent advances in understanding moiré ferroelectricity through experiments from three connected perspectives. The first perspective concerns the origin of moiré-scale polarization, with emphasis on local stacking, interfacial charge redistribution, lattice reconstruction and strain-related effects. Then it discusses polarization switching and domain-wall dynamics, including interlayer sliding, domain-wall motion, mechanical perturbation, pinning and engineered multilayer stacking. Finally, it considers the formation and identification of topological polar textures, where ordinary polar-domain networks must be distinguished from topologically structured polar order. Across these topics, the understanding of moiré ferroelectricity has advanced together with characterization methods. Structural, electrostatic, optical, electromechanical and operando

measurements provide complementary information on local stacking, potential landscapes, domain evolution and switching pathways [33]. This combined view is essential for moving the field from phenomenological observation toward predictive control, programmable polar landscapes and moiré ferroelectric devices [40–42].

2. Polarization Origin

Polarization in moiré ferroelectrics is governed by a multiscale hierarchy that couples atomistic symmetry breaking, mesoscale lattice reconstruction and macroscopic field response. At the atomic scale, local stacking registry defines the elementary interfacial dipoles, whose origin varies across material platforms. Polarization at hexagonal boron nitride and transition metal dichalcogenide interfaces mainly arises from stacking-dependent spatial charge redistribution, whereas conducting moiré platforms are dominated by electronically driven polar order. At the mesoscale, the competition between interlayer adhesion and intralayer elasticity drives the reorganization of local dipoles into reconstructed polar domains and domain-wall networks. These domain walls and saddle-point regions are not merely passive boundaries. They can host in-plane polar components, strain gradients and flexoelectric responses, and under specific symmetry conditions, they can further generate topological polar textures. At the macroscopic scale, the reconstructed polar landscape determines field-driven polarization switching pathways, domain-wall dynamics and macroscopic optoelectronic responses. Moiré ferroelectricity is therefore a deeply coupled system, in which stacking-induced interfacial polarity is reorganized by lattice relaxation, modulated by electromechanical coupling and related effects, and finally manifested macroscopically through mesoscale domain dynamics.

2.1. Microscopic Basis of Moiré Ferroelectricity

In conventional displacive ferroelectrics, polarization reversal is generally mediated by ionic displacement within the crystallographic unit cell [43]. In contrast, van der Waals interfaces exhibit a distinct switching paradigm, in which out-of-plane polarity is governed by interlayer translation, local stacking registry and moiré reconstruction. Early electrical transport, charge-sensing, piezoresponse force microscopy (PFM), Kelvin probe force microscopy (KPFM) and structural measurements established this stacking-controlled polarization response [14,23]. Graphene/hBN moiré heterostructures revealed an unconventional polarization response associated with electronic reconstruction in moiré minibands [19]. Bilayer hBN and sliding van der Waals interfaces identified interlayer sliding as a structural switching coordinate for out-of-plane polarization [13,16]. Rhombohedral-stacked and marginally twisted transition metal dichalcogenide (TMD) bilayers further showed that stacking-dependent interfacial polarity can be organized into switchable polar-domain networks [14]. These findings reframed the central question from whether van der Waals interfaces can host switchable polarity to how stacking-symmetry breaking, electronic redistribution and lattice reconstruction collectively generate the measured macroscopic polarization response.

The microscopic basis of this coupled mechanism lies in the atomistic stacking-polarity relation. In hBN and TMD interfaces, the dominant contribution to polarization is not a large vertical ionic displacement. Instead, local inversion- or mirror-symmetry breaking at specific stacking registries induces asymmetric interlayer orbital hybridization and stacking-dependent charge redistribution, thereby producing an elementary out-of-plane interfacial dipole [13,14]. In bilayer hBN, as shown in Figure 2a(i), inversion-related AB and BA stackings carry opposite polarities and can be interconverted by in-plane translation [13,16]. Similarly, in rhombohedral-stacked TMD bilayers, local MX and XM registries generate interlayer potentials with opposite signs [14]. Conductive interfacial ferroelectrics further show that such atomically confined polar interfaces can contribute cumulatively even in carrier-rich environments, indicating that interfacial dipoles are not completely suppressed by free-carrier screening [44]. Together, these results define the local microscopic origin of polarity in structurally governed sliding and interfacial ferroelectrics.

The second level of the mechanism concerns the mesoscale organization of local dipoles within the moiré lattice. A small twist angle introduces competition between interlayer van der Waals adhesion and intralayer lattice elasticity. This competition drives the expansion of energetically favored local stacking configurations and reorganizes the polar distribution into reconstructed domains and domain-wall networks. In marginally twisted hBN, electrostatic imaging resolved charge-polarized triangular superlattices associated with periodically alternating local stackings [23]. In marginally twisted TMD bilayers shown in Figure 2a(ii), combined structural characterization and electrostatic probing demonstrated that stacking-dependent local polarity is reorganized into long-range polar-domain networks [14]. Theoretical and network models further indicate that the morphology of these polar networks and their field tunability are governed by the interplay among interlayer adhesion, intralayer elastic cost and electrostatic energy [17,18]. Thus, the key issue in moiré ferroelectricity is not only the microscopic

formation of elementary interfacial dipoles, but also their reconstruction through lattice relaxation into mesoscale polar textures. This multiscale framework motivates the use of the local structural, electrostatic, optical and operando probes.

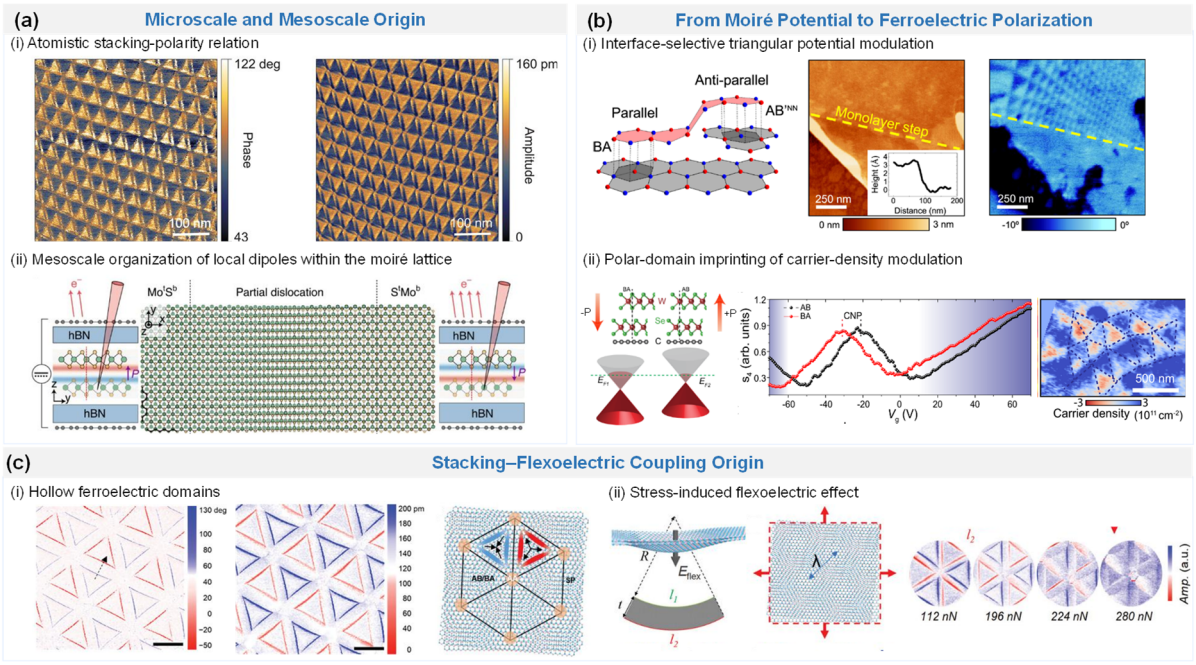

Figure 2. Multiscale origin of moiré ferroelectric polarization. (**a**): (**i**) Vertical PFM phase and amplitude images reveal stacking-dependent out-of-plane polarization and distinct domain-wall response in twisted bilayer BN. Copyright 2021, American Association for the Advancement of Science [16]. (**ii**) Mirror-related stacking domains with opposite charge transfer separated by partial dislocations in marginally twisted MoS_2. Copyright 2022, Springer Nature [14]. (**b**): (**i**) Dc-EFM detects triangular potential modulation only on the polar-aligned side, distinguishing charge-polarized interfacial superlattices from generic moiré contrast in marginally twisted hBN. Copyright 2021, Springer Nature [23]. (**ii**) Alternating polar domains in twisted WSe_2 produced domain-dependent Fermi-level shifts, distinct charge-neutrality points and nanoscale carrier-density modulation. Copyright 2023, Springer Nature [33]. (**c**): (**i**) PFM phase and amplitude images reveal hollow triangular polar domains. Strain-gradient-induced flexoelectric fields redistribute polarization charges toward reconstructed domain boundaries in marginally twisted hBN. (**ii**) Stress-induced flexoelectric effect. Copyright 2024, Wiley-VCH [39].

2.2. Identifying Ferroelectric Polarization from Moiré Potentials

Building on the multiscale stacking-polarity relation established above, a key challenge is to determine when a periodic moiré potential can be assigned to ferroelectric polarization. This distinction is essential because moiré potentials can also arise from periodic interlayer coupling, lattice corrugation, dielectric modulation or nonpolar electrostatic reconstruction. Near-60° twisted BN provides a useful boundary case. Although the periodic substrate potential can reconstruct the band structure of an adjacent electronic layer, the antiparallel H-stacked configuration restores inversion symmetry and therefore precludes spontaneous out-of-plane ferroelectric polarization [45]. Twisted trilayer WS_2 gives a second cautionary example. Scanning tunneling spectroscopy resolves a deep moiré potential, but the additional top layer modifies interlayer coupling and promotes charge delocalization across the trilayer, suppressing the layer-polarized dipole order expected from an asymmetric bilayer stacking [46]. These examples show that local probes must distinguish electrostatic moiré modulation from a switchable polarization order tied to interfacial symmetry breaking.

Correlated structural and electrostatic measurements provide the experimental basis for this distinction. In marginally twisted hBN, electrostatic force microscopy resolved triangular domains with alternating surface potentials, assigning the local contrast to reconstructed interfacial dipoles rather than to a generic moiré modulation (Figure 2b(i)) [23]. In marginally twisted MoS_2, backscattered-electron channeling contrast imaging and KPFM identified the same reconstructed network through structural and electrostatic channels [14]. Four-dimensional scanning transmission electron microscopy further showed that polar domains in van der Waals ferroelectrics are coupled to in-plane strain and out-of-plane stacking order [47]. These studies demonstrate that polarization

assignment requires correlated evidence from registry, relaxed structure and calibrated local potential, rather than electrostatic contrast alone.

Once a polar network is established, its electrostatic field can be imprinted onto adjacent 2D layers. In twisted hBN, the electrostatic moiré potential was quantitatively linked to interfacial charge redistribution and was shown to depend on both the distance from the twisted interface and the moiré supercell size [32]. Tunable twisted hBN structures further demonstrate that the strength and geometry of the superlattice potential can be adjusted through twist angle, interface design and multilayer polarization accumulation [48]. Twisted BN substrates provide a closely related example of electrostatic imprinting. Periodic up- and down-polarized domains in the BN substrate can impose a remote superlattice potential on adjacent bilayer graphene, producing satellite resistance peaks and Hofstadter-type band-structure signatures [45]. Remote moiré ferroelectricity in twisted WSe_2 similarly shows that a polar superlattice can modulate a separated graphene transport layer through long-range electrostatic coupling [34]. These results place moiré ferroelectrics in a broader role. They are not only polar domain textures, but programmable electrostatic substrates that can reshape the electronic structure of nearby functional layers.

Plasmonic and photocurrent readouts follow the same physical principle. The alternating out-of-plane polarization generates a spatially periodic electrostatic potential, which modulates the local carrier density and Fermi level of a neighboring graphene sheet. In graphene/twisted-WSe_2 structures, near-field infrared nano-imaging visualized the ferroelectric domain pattern through the graphene plasmonic response, while nano-photocurrent measurements detected domain-dependent optoelectronic signals [33] (Figure 2b(ii)). In graphene on twisted hBN, scanning tunneling microscopy showed that the moiré ferroelectric potential can generate periodic quantum confinement, and local tip manipulation can modify ferroelectric polarization near moiré boundaries [49]. Plasmonic polarization sensing provides another high-sensitivity route, using graphene plasmons to detect electrostatic superlattice potentials generated by adjacent polar domains [50]. These methods should be treated as functional readouts rather than direct atomic-scale proof of the switching pathway. Their value lies in translating buried polar domains into measurable carrier-density, plasmonic and photocurrent responses.

Excitonic probes provide a parallel readout channel in semiconducting monolayers. When monolayer $MoSe_2$ is placed near a twisted hBN ferroelectric substrate, the periodic electrostatic potential modifies the local carrier environment and reshapes exciton-polaron states [51]. Hyperspectral photoluminescence and KPFM measurements show that the twisted hBN (t-hBN) polar domains can imprint spatially varying potentials onto $MoSe_2$, leading to domain-dependent excitonic responses [51]. Related optical measurements further show that moiré ferroelectricity can modulate light emission from a semiconductor monolayer through the electrostatic potential generated by the twisted hBN substrate [40]. Electrostatic moiré superlattices can also confine excitons by creating strong local fields near polar domain boundaries, providing an optical signature of the same electrostatic landscape [52]. These optical studies reinforce the concept of electrostatic imprinting. The polar texture is not only visible in local potential maps, but also in the excitonic energy landscape of an adjacent semiconductor.

Moiré ferroelectricity can also act as an active switch for correlated electronic states. In Td-WTe2/H-WSe2 superlattices, vertical-field-driven ferroelectric reversal changes the polarization-dependent charge transfer between the two WTe_2 monolayers [24]. Because the interfacial WTe2 layer experiences a stronger moiré potential from WSe_2, this charge redistribution changes the effective moiré potential depth and switches insulating states at integer fillings [24]. The same ferroelectric reversal redistributes the Berry-curvature dipole and enables control of the nonlinear anomalous Hall response [24]. This example moves beyond static readout. It shows that a switchable ferroelectric polarization state can serve as a nonvolatile control parameter for moiré band filling, correlated insulation and nonlinear transport. In conclusion, assigning the origin of polarization in moiré ferroelectrics requires verifying the consistency among local symmetry breaking, reconstructed stacking domains, calibrated electrostatic contrast and switchable response within the same real-space texture.

2.3. Coupled Mechanisms of Moiré Ferroelectric Polarization

Moiré ferroelectric polarization originates from the multiscale coupling among stacking-dependent interfacial dipoles, lattice relaxation, electronic screening and electromechanical coupling. In hBN- and TMD-based moiré systems, stacking-dependent interfacial dipoles must be converted into measurable, switchable and tunable polar landscapes through lattice reconstruction, electronic screening and electromechanical coupling. Lattice relaxation determines the reconstruction of local stacking domains and the morphology of domain-wall networks. Electronic screening modulates the measurable strength of the local electrostatic potential, while atomic-scale relaxation affects the correspondence between local dipoles and domain morphology. Ferroelectric polarization in conducting moiré systems requires separate consideration as an independent mechanism. In graphene/hBN, monolayer graphene moiré superlattices and hBN-encapsulated monolayer graphene, moiré

minibands, carrier redistribution and electronic reconstruction can participate in the formation of switchable polarization states [19,53,54]. Such electronically driven polar order is distinct from the modulation of interfacial-dipole readout by carrier screening. In conductive interfacial ferroelectrics, mobile carriers can coexist with atomically localized interfacial dipoles and modify the screening condition and readout form of polarization [29,44]. In double-moiré systems, correlation-modulated screening can coexist with signatures of flexoelectric polar vortex structures, suggesting that electronic reconstruction, carrier screening and strain-induced polar textures may become coupled in complex moiré environments [55].

When local dipoles are embedded in small-angle moiré superlattices, their polarization response is governed by domain reconstruction, domain-wall migration and external-field control. An applied electric field can modify the relative stability of oppositely polarized domains and redistribute the domain-wall network [26]. The theory of polar domains further distinguishes local polarization, macroscopic ferroelectric hysteresis and field-driven domain-wall motion, indicating that polar moiré domain patterns must be evaluated together with specific switching pathways [27]. The measured polarization is the net response of a reconstructed polar texture, controlled by domain area fraction, domain-wall width, strain field and pinning landscape. In lattice-mismatched TMD heterobilayers, atomic reconstruction barriers restrict the evolution of local stacking preference into extended polar-domain networks [56].

In moiré ferroelectrics, strain gradients constitute a key electromechanical channel that links lattice reconstruction to polar textures. Local relaxation near domain walls, saddle-point regions and reconstructed boundaries can generate strain gradients and thereby modulate electromechanical response and polar-domain morphology. In marginally twisted hBN, stacking ferroelectricity and flexoelectricity are coupled, allowing strain gradients to reshape the local electromechanical contrast and polar-domain structure [39] (Figure 2c). Through nanoscale flexoelectric domain engineering, strain-gradient coupling can also enable reversible writing and erasure of local polar states [57]. In twisted moiré superlattices, engineered strain fields can stabilize remanent polarization and regulate antiferroelectric-like responses in moiré domain networks [58]. Flexoelectricity therefore acts as an internal electromechanical channel that couples reconstructed strain fields to both in-plane and out-of-plane polarization components.

Electromechanical coupling endows polar textures in moiré ferroelectrics with a full vector character. Theoretical predictions show that strained and twisted bilayers can host polar meron-antimeron networks when the polarization vector rotates continuously along reconstructed domain-wall networks [30]. A recent decomposition framework for polarization textures in moiré homo- and heterobilayers further indicates that alternating out-of-plane polarization and in-plane Néel- or Bloch-like components can be derived from local sliding configurations, thereby linking stacking ferroelectricity to vector polar textures [59]. Large-scale modelling of hBN moiré superlattices shows that lattice mismatch and vertical electric fields can tune topological polarization patterns in large moiré supercells [60]. These theoretical results are consistent with experimental reports of lateral polar networks, confined interfacial polar textures, anomalous vector-PFM patterns and edge-related polarization topology in hBN and TMD moiré systems [25,38,61,62]. In this mechanistic picture, strain concentration at domain walls and saddle-point regions activates flexoelectric and piezoelectric couplings and generates in-plane polarization components. The resulting vector field can rotate within the moiré unit cell, producing meron-like or other topologically non-trivial polar configurations.

Edges and domain walls further influence the stability and evolution pathways of polar textures. In interfacial ferroelectrics, moiré edges can undergo reversible structural phase transitions, while local force and strain can reshape stacking registry, edge geometry and domain-wall evolution [63]. Domain-wall type, mobility and reversibility can alter the stability of interfacial polar states and affect polarization switching pathways [31]. The formation and evolution of polar textures are therefore jointly controlled by boundary geometry, domain-wall type, local strain and mechanical perturbation.

Twist angle, layer number and stacking sequence further determine the organization of polar landscapes. For WSe_2 bilayers, twist angle regulates the competition between net ferroelectricity and antiferroelectric-like domain organization, while domain-wall-network connectivity constrains field-driven polar transitions [35,64]. Rotationally engineered multilayers introduce additional interfaces and switching pathways, making layer number and stacking sequence important variables for interfacial-polarization control [36]. The observable polarization is jointly determined by local stacking polarity, the number of polar interfaces, interfacial registry and domain-wall connectivity. The moiré ferroelectric response arises from the coupling of multiple mechanisms, whose relative contributions are strongly platform-dependent. Future studies need to integrate first-principles charge analysis, atomically resolved structural mapping, calibrated local-potential measurements, vector-polarization imaging and operando switching probes within the same device to distinguish the specific roles of interfacial charge redistribution, electronic order, screening, lattice relaxation, electromechanical coupling and domain-wall reconstruction.

3. Polarization Switching and Domain-Wall Dynamics

Moiré ferroelectric switching should be understood through the coupled evolution of local stacking configurations, domain-wall networks and lattice reconstruction. Early studies established switchable interfacial polarization in moiré, interfacial and sliding ferroelectric systems mainly through electrical hysteresis and static scanning-probe measurements. In graphene/hBN moiré heterostructures, experiments reported an unconventional ferroelectric response associated with moiré-scale electronic reconstruction and interfacial symmetry breaking [19]. In marginally twisted hBN, electrostatic measurements resolved charge-polarized interfacial superlattices composed of alternating BN and NB stacking domains [23]. In stacking-engineered bilayer hBN, the out-of-plane polarization direction can be selected by interlayer stacking registry [16]. This static picture was then extended to broader van der Waals platforms. Interfacial ferroelectricity induced by van der Waals sliding established relative interlayer translation as a polarization-switching coordinate [13]. In rhombohedral-stacked TMD bilayers, inversion-symmetry-broken semiconducting interfaces can likewise host switchable out-of-plane polarization [14]. Marginally twisted two-dimensional semiconductors further introduced reconstructed polar-domain networks, where alternating domains and field-driven domain walls emerge within twist-angle-controlled moiré patterns [14] (Figure 3a(i)). These results established a static stacking-polarity mapping and raised the problem of identifying the switching pathway. Reversible polarization signals alone are insufficient to distinguish among interlayer sliding, local stacking conversion, domain-wall propagation, dislocation rearrangement and soliton-network reconstruction.

These static observations naturally lead to the dynamical mechanism of polarization reversal. In reconstructed moiré superlattices, polarization reversal is constrained by locally stable stacking domains and domain-wall networks. Once elastic relaxation partitions the interface into locally stable stacking domains, macroscopic switching proceeds through the migration and reconstruction of local domain boundaries. Network models of twisted TMD bilayers attribute the equilibrium domain pattern to the competition among stacking energy, elastic deformation and electrostatic energy [18]. The theory of polar domains in moiré heterostructures further distinguishes local polar textures, macroscopic ferroelectric hysteresis and field-driven domain-wall motion as related but physically distinct processes [27]. Electrically tunable stacking-domain models show that an external field changes the relative energy of adjacent stacking domains and drives the expansion of the energetically favored domain [26]. This picture is also consistent with the general dynamics of ferroic switching. Polarization reversal in conventional ferroelectrics usually involves reverse-domain nucleation, domain growth and domain-wall motion, as systematically discussed in $PbTiO_3$ and $BaTiO_3$ [65]. In ferroelectric domain-wall nanoelectronics, domain walls are regarded as functional entities with distinct structural and electronic properties [66]. In sliding ferroelectrics, nonvolatile polarization switching in 3R-MoS_2 can be achieved through domain-wall release and large-domain sliding [67]. Thus, the key dynamical variables in reconstructed moiré systems are the migration and reconstruction of local domain boundaries. Within this domain-wall-centered picture, operando electron microscopy provides direct real-space evidence. In twisted WSe_2 homobilayers, operando imaging directly tracked the field-driven evolution of polar-domain networks and revealed that domain-wall-network topology constrains the transition between moiré-domain antiferroelectric and ferroelectric states [35]. Domain walls, dislocations and soliton-like reconstruction boundaries thereby emerge as active structural units that mediate local stacking conversion and polarization reversal.

3.1. In Situ Visualization and Dynamic Probes of Polarization Reversal

The dynamic pathways of polarization reversal in moiré ferroelectrics require joint analysis through operando imaging, local manipulation and indirect dynamical readouts. Operando electron microscopy provides the most direct real-space evidence for polarization reversal in reconstructed moiré ferroelectrics. In twisted WSe_2 homobilayers, Ko et al. tracked field-driven polar-domain evolution and showed that the transition from a moiré-domain antiferroelectric state to a ferroelectric state is governed by the topology and connectivity of the domain-wall network [35]. Under strong electric fields, neighboring domain walls can merge into topologically protected perfect dislocations after collision, thereby constraining the global moiré-domain antiferroelectric (MDAF)-to-ferroelectric (FE) transition. This process identifies the domain-wall network as the operative dynamical structure for field-driven switching. The same study resolved rapid domain-wall motion with velocities reaching hundreds of micrometers per second. Disorder-induced pinning and depinning also produced Barkhausen-like discontinuities in the polarization response. Van Winkle et al. further extended this operando framework to WSe_2 multilayers, showing that engineered interlayer rotations can tune the spatial organization and switching dynamics of polar domains. Distinct trilayer configurations produce either global or local switching, together with strain-biased coercive responses [36]. Field-driven polarization reversal is therefore jointly controlled by domain connectivity, boundary constraints and local lattice conversion.

Local probes and mechanical manipulation further reveal the structural carriers of this switching pathway. In marginally twisted WS_2 bilayers, Molino et al. used scanning tunneling microscopy to image and manipulate partial-dislocation networks at symmetry-broken interfaces [68]. As shown in Figure 3a(ii), the STM tip field induced elastic bending of partial screw dislocations and, at critical fields, drove their merger into perfect screw dislocations. This process corresponds to the local expulsion of unfavorable polar domains and the reconstruction of interfacial stacking registry, indicating that polarization switching is mediated by mobile partial dislocations and domain walls. Local mechanical stimulation provides another route for switching control. The local force exerted by an AFM tip can induce interlayer sliding in interfacial ferroelectrics, directly coupling nanoscale stress to stacking-registry conversion and polarization reversal [37]. In moiré-edge geometries, local pressure can drive a convex-to-concave boundary transition, accompanied by local sliding and the splitting of a single domain wall into multiple domain-wall segments [63]. Heterostrain can further distort regular triangular moiré cells into irregular supercells or stripe-like domains. Under mechanical perturbation, these distorted units may migrate asymmetrically, with displacement directions not necessarily parallel to the applied shear and in some cases nearly perpendicular to it. PFM/AFM-based local writing and flexoelectric-domain manipulation also show that nanoscale stress gradients can reversibly write and erase polar configurations in van der Waals ferroelectrics [57]. Local stress, heterostrain, defect pinning and moiré-edge geometry therefore constitute intrinsic variables in the switching landscape.

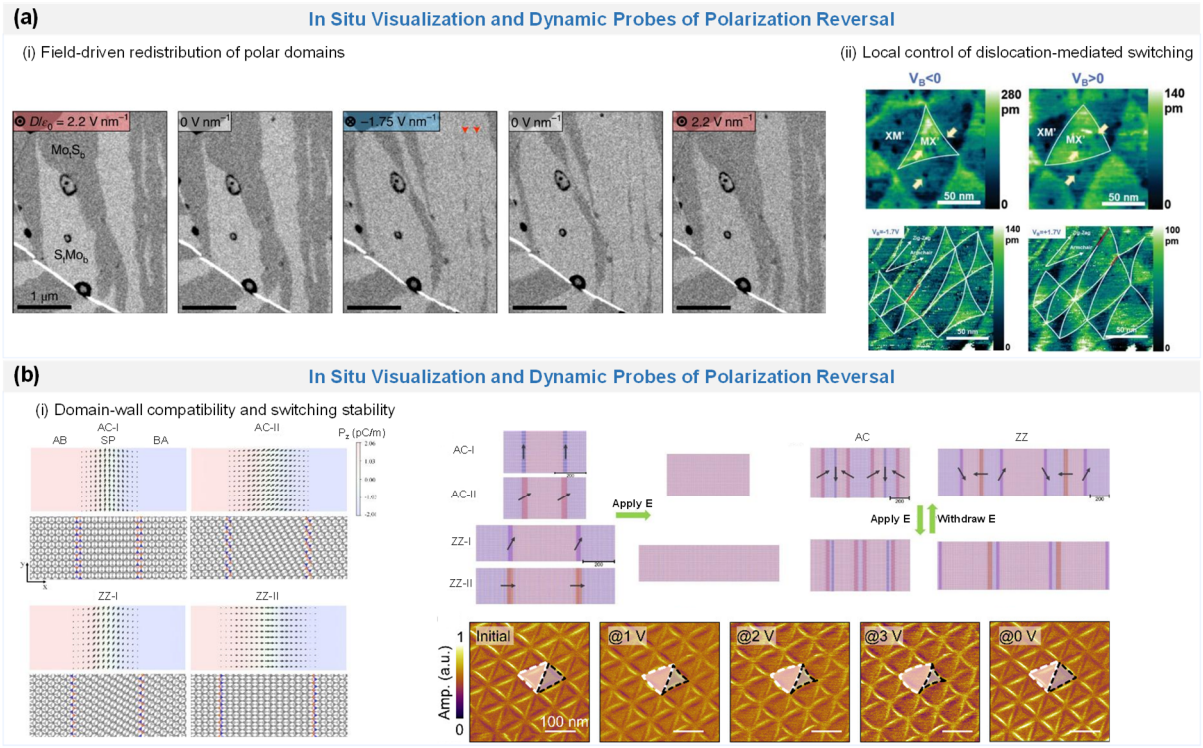

Figure 3. Polarization switching and domain-wall-network dynamics in moiré ferroelectrics. (**a**): (**i**) BSECCI imaging under transverse electric fields shows reversible redistribution of polar domains in marginally twisted MoS_2. Copyright 2022, Springer Nature [14]. (**ii**) STM imaging under opposite local electric displacement fields shows reversible bending of domain walls. In elongated domains, the wall geometry evolves into a reconstructed double-wall configuration. Copyright 2023, Wiley-VCH [68]. (**b**) Atomic models distinguish AC- and ZZ-type domain walls with different in-plane polarization directions. Wall type and network compatibility determine whether domains collapse into a single-polar state or recover after field removal. Adapted with permission from [31] Copyright 2026 American Chemical Society.

Spectroscopic and transport signatures provide indirect but mechanism-resolved evidence for soliton-network evolution during polarization reversal. In bilayer MoS_2 nanostructures with reconstructed moiré superlattices, Li et al. observed ferroelectric hysteresis together with Raman signatures of soliton disentangling and lattice viscosity [69]. The key spectroscopic feature is the splitting and hysteretic evolution of the in-plane E_{2g} phonon mode. This splitting reflects local strain accumulation in one-dimensional moiré solitons and the breaking of threefold rotational symmetry during reconstruction. Under a vertical displacement field, the evolution of the E_{2g} mode provides a vibrational fingerprint of reversible soliton disentangling, re-entangling and lattice relaxation.

In marginally twisted hBN, stacking ferroelectricity and flexoelectricity are intertwined, allowing strain gradients to reshape the local polarization response of the moiré superlattice [39]. These readouts indicate that switching is accompanied by strain redistribution, soliton-network reconstruction and lattice-viscosity-limited relaxation.

The dynamic evidence above reveals the dependence of moiré ferroelectric switching on twist angle, heterostrain and boundary conditions. In WSe_2 bilayers, twist-angle variation can tune the polar-network morphology and the associated ferroic response [61]. In twisted hBN, local STM manipulation can couple domain-wall displacement to electronic superlattice potentials and quantum confinement in an adjacent graphene layer [49]. Moiré ferroelectric switching therefore depends strongly on both material platform and structure.

3.2. Domain Walls as Active Switching Units

Domain-wall-mediated switching is a key mechanism for understanding polarization reversal in moiré and sliding ferroelectrics. In these systems, domain walls are dynamic sites where local symmetry breaking enables polarization reversal. Within a single commensurate domain that preserves C_3 rotational symmetry, an out-of-plane electric field cannot efficiently generate the in-plane force required for collective interlayer translation. At a domain wall, the reduced local symmetry allows the off-diagonal components of the Born effective charge tensor to convert the vertical electric field into an in-plane driving force for local stacking-registry change [70]. This tensorial electromechanical coupling explains why polarization reversal can proceed along domain walls. In related sliding-ferroelectric systems, the superlubric propagation of wavelike domain walls further indicates that pre-existing wall-like structures can provide low-dissipation and fast switching channels, with simulated room-temperature velocities approaching 4.0×10^3 m s^{-1} and an anomalous cooling-enhanced switching speed [71].

The switching function of domain walls is also closely related to their internal polarization topology. In reconstructed moiré ferroelectrics, saddle-point stacking regions inside domain walls can host pronounced in-plane polarization components [61]. Polarization-field reconstruction based on vector PFM shows that these in-plane components couple to alternating out-of-plane polarization and generate vortex-like polar textures near domain walls [25]. Depending on the relative orientation between the in-plane polarization vector and the domain-wall direction, the polar rotation can exhibit Bloch-type or Néel-type character and organize into meron-antimeron-like networks [25]. Domain-wall type further constrains the local sliding energy landscape and stacking-conversion pathway. As shown in Figure 3b, AC-I, AC-II, ZZ-I and ZZ-II domain walls differ in width, energy and elastic compatibility [31]. In single-type domain-wall networks, field-driven domain-wall motion can merge neighboring walls into a single-domain configuration. In mixed-type networks, elastically incompatible wall segments are difficult to annihilate completely, and the system tends to recover the moiré-domain antiferroelectric ground state after removal of the field [31]. The switching pathway is therefore jointly selected by the energy difference between adjacent domains, the topological compatibility of the wall network and elastic compatibility.

This compatibility constraint determines whether domain-wall switching exhibits volatile, nonvolatile or multistate behavior. In an ideal defect-free mixed-type network, an out-of-plane electric field can expand high-energy saddle-point regions and produce finite net polarization. After the field is removed, the system returns to the topologically protected moiré-domain antiferroelectric state [31]. Local structural perturbations can suppress the retreat of high-energy domain-wall configurations and stabilize field-written polar states [31]. Moiré-edge phase transitions can transform convex boundaries into concave ones, redirect domain-wall trajectories and suppress spontaneous back-switching under local mechanical loading [63]. Heterostrain gradients can distort the ideal triangular domain network and create anisotropic pathways for domain-wall migration [39]. In nanoscale flexoelectric domain engineering of two-dimensional $CuInP_2S_6$, stress gradients can reversibly write and retain local polar configurations [57]. Defects, strain gradients, edge geometry and local mechanical perturbations therefore jointly shape the migration barriers of domain walls. Random pinning increases switching inhomogeneity, whereas controlled pinning can stabilize selected domain-wall configurations, suppress spontaneous back-switching and support deterministic multistate nonvolatile responses.

For practical devices, domain-wall pathways, pinning barriers and heterostrain distributions directly affect switching voltage, reversal speed, retention, fatigue behavior and multistate consistency [18,26,27,35,36,39]. Device design should therefore consider the cooperative control of local domain-wall trajectories, defect pinning, edge geometry and strain fields. Heterostrain can modulate domain-wall migration pathways and local switching barriers, thereby affecting the abruptness or gradualness of device response [35,36,39]. More uniform domain-wall motion is favorable for digital switching with low device-to-device variability, as suggested by deterministic one-dimensional domain-wall motion and highly reproducible multistate polarization switching in sliding-ferroelectric systems [70]. Distributed pinning and multibarrier depinning processes may instead produce gradual responses. Barkhausen-like discontinuities observed by operando imaging indicate that domain-wall pinning-

depinning strongly affects the switching pathway. Random defects generally increase coercive-field dispersion and reduce device uniformity, whereas designed pinning sites, edge structures and strain gradients can stabilize selected domain-wall configurations, suppress spontaneous back-switching and enhance nonvolatile retention [31,63]. This insight motivates future device studies to establish quantitative correlations among domain-wall-network architecture, local strain fields, pinning barriers and macroscopic electrical metrics.

4. Topological Polar Textures

4.1. Identification of Topological Polar Textures

Ordinary moiré polar domains are primarily defined by stacking-dependent out-of-plane polarity and scalar domain contrast, whereas topological polar textures are defined by the non-trivial spatial configuration of a reconstructed polarization vector field. In sliding ferroelectrics and stacking-engineered ferroelectrics, AB/BA stacking domains can produce periodic out-of-plane polarization reversal and scalar-like polar contrast [13,14,16]. Such contrast establishes local polarity, while topological polar textures require coupling between in-plane and out-of-plane polarization components, local rotation across domain walls or saddle-point regions, and possible winding structures or meron-antimeron-like configurations [25,30,38] (Figure 4a). In reconstructed moiré superlattices, local stacking registry determines the sign of the out-of-plane interfacial dipole, while lattice relaxation organizes these dipoles into triangular or network-like domain structures [13,14,17]. Near domain walls and saddle points, continuously varying local interlayer translation reduces local symmetry and introduces in-plane polarization components in addition to out-of-plane polarization reversal [30,72].

Bennett et al. predicted meron-antimeron networks in strained or twisted bilayers with broken inversion symmetry [30]. In their model, the in-plane polarization component couples with alternating out-of-plane polar domains, making the total polarization field topologically non-trivial. In this model, the winding number describes the rotation of the in-plane polarization around a texture. The Bloch-like and Néel-like labels describe different orientations of the in-plane component, with tangential and radial rotation patterns, respectively. Li et al. used vector PFM to map both out-of-plane and in-plane piezoresponse in marginally twisted hBN, $MoSe_2$ and WSe_2 [25]. Their results resolved alternating out-of-plane polar domains together with vortex-like in-plane polarization near moiré domain walls. Therefore, vortex-like polar textures should be identified from resolved or reconstructed in-plane vector rotation, rather than from scalar contrast alone. Pan et al. combined PFM polar mapping with STEM atomic-displacement mapping in twisted boron nitride [38]. This correlation links topological polar textures to interfacial sliding, local lattice reconstruction and displacement fields.

This theoretical picture requires further experimental validation. Periodic triangular domains, PFM phase reversal, KPFM potential contrast, transport hysteresis and optical contrast can support stacking-dependent polarity or electrostatic modulation [23,33]. Topological assignment further requires the identification of in-plane and out-of-plane polarization coupling, domain-wall-localized rotation, chirality or winding structures. In marginally twisted hBN, WSe_2 and $MoSe_2$, vector PFM has reconstructed alternating out-of-plane polarization and vortex-like in-plane polarization near domain walls [25]. The combination of PFM and STEM atomic displacement mapping further links topological polar textures in twisted boron nitride to interfacial displacement fields and local structural reconstruction [38]. Therefore, experimental identification of topological polar textures should further integrate polarization vector-field reconstruction, atomic displacement mapping and correlative local structural characterization.

4.2. Vector Polar Textures

Experimental confirmation of topological polar textures requires vector-resolved polarization mapping and structural correlation where possible. Vector PFM can reconstruct coupled out-of-plane and in-plane electromechanical responses, and PFM combined with STEM displacement mapping can connect these responses to interfacial sliding and local lattice reconstruction [25,38]. 4D-STEM or strain-resolved electric-field mapping can add direct information on in-plane fields and nanoscale strain linked to vortex-like polar textures [73]. By contrast, KPFM and EFM provide local potential contrast, while single-channel out-of-plane PFM probes the out-of-plane electromechanical response. SHG, PL, plasmonic imaging, photocurrent and transport serve as functional readouts of symmetry breaking, electrostatic modulation or device response. These indirect signals support polar domains or moiré potentials, but they cannot by themselves establish vortex, meron, antimeron, winding, Bloch-type or Néel-type topology [33,34,40,74,75].

Vector PFM provides a key route for identifying topological polar textures by resolving coupled out-of-plane and in-plane electromechanical responses. Li et al. used vector PFM to reconstruct the polarization field in R-type marginally twisted hBN, where domain regions exhibit alternating out-of-plane polarization and domain walls host

vortex-like in-plane polarization patterns [25]. Similar polar textures were also observed in marginally twisted $MoSe_2$ and WSe_2 homobilayers, indicating that the coupled evolution of in-plane and out-of-plane polarization components across moiré domain-wall networks can serve as important evidence for polar topology [25].

Correlative atomic-structure characterization provides another critical line of evidence. Pan et al. combined microscopic polarization mapping by PFM with STEM atomic displacement mapping to study topological polar textures in twisted boron nitride [38]. As shown in Figure 4b, PFM resolves the local polarization response, while STEM displacement mapping directly reveals the atomic displacement field at the moiré interface, thereby linking topological polar textures to continuous interlayer sliding, local lattice reconstruction and domain-wall displacement [38]. This work further shows that the topological polar texture is confined to the twisted interface and can be manipulated nonvolatilely [38].

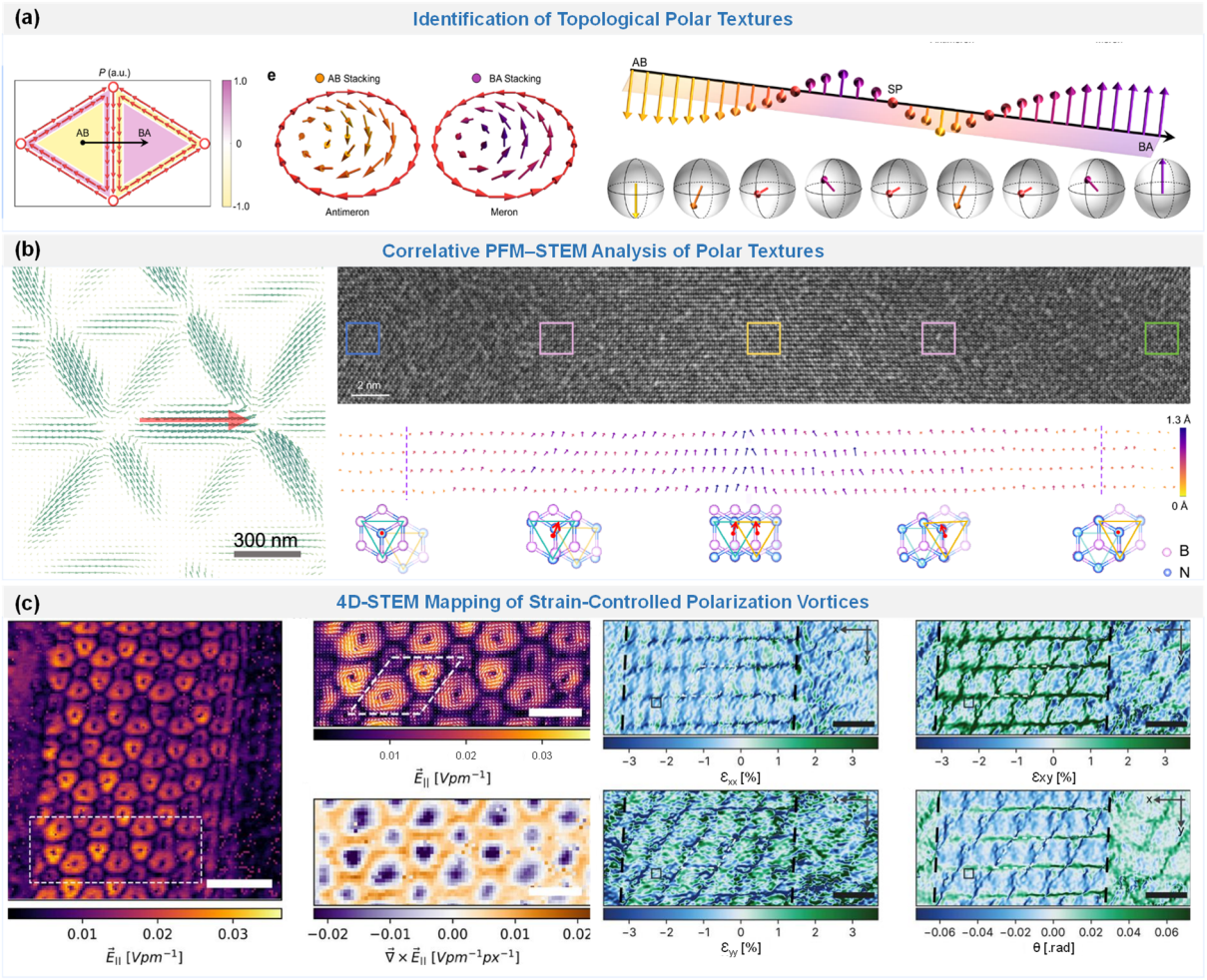

Figure 4. (**a**) Polar-vector topology in twisted hBN. The polarization rotates across the wall, forming meron-antimeron-like textures on a ferroelectric Bloch sphere. Copyright 2025, Springer Nature [25]. (**b**) Correlative mapping of polarization and atomic displacement. LPFM vector mapping resolves curling in-plane piezoresponse within the triangular moiré texture. Copyright 2025, Springer Nature [38]. (**c**) 4D-STEM mapping of strain-controlled polarization vortices. In-plane electric-field maps resolve vortex-like polar textures within the moiré unit cell. Copyright 2025, Wiley-VCH [73].

Optical and transport methods mainly provide functional readouts. SHG probes inversion-symmetry breaking and stacking-related symmetry changes. Exciton-enhanced near-field SHG has been used to image nanoscale stacking order in bilayer WSe_2, showing that nonlinear optical responses can probe local symmetry and structure-property relationships at nanometer length scales [74]. In hBN moiré homobilayers, theoretical SHG analysis further indicates that atomic relaxation lowers the symmetry of the moiré structure and modifies the expected SHG response [75]. In graphene/twisted-WSe_2 structures, near-field infrared nano-imaging and nano-photocurrent measurements visualize moiré ferroelectric domains through the graphene plasmonic response and local photocurrent modulation [33]. Ferroelectric moiré domains in twisted hBN can modulate the light emission of an adjacent $MoSe_2$ monolayer through surface electrostatic potentials [40]. Remote moiré ferroelectric potentials

generated by twisted WSe_2 can also be imprinted onto bilayer graphene and used to tune its band structure and transport response [34].

In conclusion, rigorous identification of topological polar textures requires both polarization-vector-field reconstruction and correlative atomic-structure evidence. Vector PFM resolves the polarization vector field, STEM displacement mapping establishes the connection between polar textures and atomic reconstruction, while SHG, plasmonic imaging, nano-photocurrent mapping, PL and transport reveal the symmetry, electrostatic modulation and functional responses of moiré polar structures.

4.3. Domain-Wall Reconstruction and Strain-Controlled Polar Topology

The formation of topological polar textures should be understood through the cooperative interplay of local stacking registry, domain-wall reconstruction, strain fields and electromechanical coupling. Domain interiors are mainly governed by stacking-dependent out-of-plane polarization, whereas domain walls and saddle-point regions involve continuous interlayer translation and reduced local symmetry. These regions can host in-plane polarization components and transform an out-of-plane domain pattern into a polarization vector field [17,18,30,72]. PFM measurements on twisted hBN show that narrow saddle-point regions can exhibit in-plane polarization, indicating that moiré boundary regions also participate in the construction of the polarization vector field [72].

Strain and piezoelectric coupling further modulate the topology of this vector field. Theoretical models show that moiré relaxation can generate piezoelectric networks and ferroelectric domain structures in twisted TMD bilayers [17,18]. Bennett et al. further showed that strained and twisted bilayers can host polar meron-antimeron networks when out-of-plane domains couple to in-plane polarization components [30]. Experimentally, Sangers et al. reported strain-induced moiré polarization vortices in twisted multilayer WSe_2, with vortex-like textures observed in regions of pronounced nanoscale strain [73] (Figure 4c). Fan et al. further showed that edge polarization topology can couple with sliding ferroelectricity in twisted hBN, indicating that edges and domain boundaries can stabilize robust vortex-like polar configurations [62].

Flexoelectricity introduces an additional level of modulation. When strain gradients, bubbles, curvature or elastic distortions modify the local electrostatic and electromechanical landscape, flexoelectricity can strongly affect moiré polar textures. Wan et al. showed that flexoelectricity is intertwined with stacking ferroelectricity in marginally twisted hBN and can reshape moiré ferroelectric patterns, including hollow-triangle-like domain morphologies [39]. Flexoelectricity therefore becomes an important factor in tuning domain geometry, periodicity and local polar contrast. These mechanisms indicate that the stability and tunability of topological polar textures depend on the coupling among the out-of-plane polar background, in-plane polarization components at domain walls and saddle points, and local strain fields. Because these factors are modulated by stacking registry, domain-wall geometry, boundary conditions and the local mechanical environment, designed heterostrain, edge geometry, interface cleanliness, local pressure and elastic reconstruction can serve as control parameters for stabilizing selected polar topologies.

4.4. Topological Polar Textures in Magnetic and Multiferroic Moiré Systems

Building on these moiré ferroelectric textures, magnetic and multiferroic moiré systems offer a natural extension because moiré reconstruction can simultaneously influence lattice relaxation, magnetic order, and electric polarization in twisted van der Waals materials [76,77]. Recent theoretical work on twisted bilayer NiI_2 reported that moiré structural relaxation and spin-driven ferroelectricity can cooperate to generate polar-magnetic topologies [78]. In monolayer NiI_2, noncollinear magnetic order induced spin-driven ferroelectric polarization. When two such layers were twisted, the resulting moiré reconstruction generated a spatially varying stacking landscape, which in turn strongly modulates both the magnetic interactions and the local electric dipoles. Near $\theta \approx 60^{\circ}$ the competition between different stacking registries and ferroelectric displacements produces periodic polar meron-antimeron networks. In these networks, the polarization vectors exhibit vortex-like and antivortex-like winding patterns across the moiré supercell [78]. Related work on twisted multiferroic NiI_2 bilayers showed that moiré-modulated magnetic frustration can stabilize topological spin textures, including $k\pi$-skyrmion lattices and nematic spin textures ordered at the moiré scale [79]. The study also showed that these skyrmion phases can be electrically controlled by an out-of-plane electric field through its coupling to moiré-induced polarization, providing a magnetoelectric route to manipulate moiré-scale topological textures [79]. From an experimental perspective, twist-controlled WSe_2 bilayers have shown room-temperature ferroelectricity that weakens with increasing twist angle within $0^{\circ} < \theta < 3^{\circ}$ and disappears for $\theta \geq 4^{\circ}$ [64]. At low temperature, 3° twisted WSe_2 further exhibits the coexistence of ferroelectricity and correlation-driven ferromagnetic ordering, indicating twist-controlled multiferroic behavior [64].

The mechanism discussed above shows that moiré polar textures are not determined by a single factor, but by the coupled evolution of stacking registry, lattice reconstruction, strain fields, electrostatic screening and domain-wall geometry. This coupling also explains why similar experimental contrasts can correspond to different physical situations in different material platforms. A periodic moiré potential, a polar-domain pattern, reversible ferroelectric switching and a topological polar texture therefore require different levels of evidence. Table 1 summarizes these evidentiary distinctions. Table 2 further compares representative moiré ferroelectric and related interfacial-ferroelectric systems, emphasizing their polarization origins, switching pathways, domain-wall behavior and functionalities.

Table 1. Distinguishing moiré potentials, polar domains, ferroelectric switching, and topological polar textures.

Criteria	Meaning	Required Evidence	Limitations
Moiré potential	Periodic electrostatic potential or band modulation tied to a moiré lattice	Local potential or band evidence from KPFM/EFM, STM, transport, optical, plasmonic, or photocurrent readout	Does not prove switchable polarization, retained polarization, or a domain-wall switching path.
Polar domains	Spatially alternating polar regions linked to local stacking or charge redistribution.	Polar contrast from PFM, EFM/KPFM, or charge sensing, supported by stacking, structure, or local-potential correlation.	Does not prove reversible ferroelectric switching or topological polar texture.
Ferroelectric switching	Field-driven reversal of polarization with hysteresis and retention.	Reversible electrical or local-probe switching, hysteresis, retention, and, where available, real-space tracking of polar-domain evolution.	Does not rule out charge trapping, screening, or contact effects without additional evidence.
Topological polar textures	Reconstructed polarization vector fields with coupled in-plane and out-of-plane components, domain-wall-localized rotation, winding, chirality, or vortex-like patterns.	Vector-resolved polarization mapping, supported where possible by STEM displacement mapping, 4D-STEM, or strain/electric-field mapping that links the vector field to lattice reconstruction.	Scalar PFM, KPFM, transport, or optical contrast alone cannot prove polarization topology.

Table 2. Representative moiré ferroelectric and related interfacial-ferroelectric systems.

Material System	Polarization Origin	Characterizations	Switching / Domain-Wall Behavior	Functionalities and Issues	Refs.
Graphene/hBN moiré heterostructures	Electronic reconstruction and charge redistribution in graphene/hBN moiré minibands or interfaces.	Transport, Hall hysteresis, capacitance, non-local graphene sensing, conductive AFM, and calculations support switchable electronic polarization.	Field-controlled reversal of electronic polarization; domain-wall motion was not directly resolved in the cited graphene/hBN studies.	Moiré electronic switching and room-temperature graphene/hBN ferroelectric response. Direct real-space domain-wall dynamics remain insufficiently resolved.	[19,53,54]
Twisted hBN and bilayer BN interfaces	Stacking-dependent AB/BA or BN/NB interfacial dipoles; lattice relaxation, screening, and flexoelectricity modify the polar landscape.	PFM, EFM/KPFM, STM, vector PFM, STEM displacement mapping, and optical or excitonic readout link polar contrast to stacking and reconstruction.	Interlayer sliding connects inverse stacking states; domain walls and saddle points can host in-plane response.	Moiré electrostatic templates for graphene and semiconductor monolayers. Quantitative separation of stacking dipoles, screening, and flexoelectric contributions remains challenging.	[13,16,25,32,40]
Rhombohedral TMD bilayers	Opposite MX/XM stackings create opposite out-of-plane interfacial dipoles.	PFM, charge-sensing field-effect geometry, and calculations support stacking-controlled polarization.	In-plane interlayer sliding reverses polarization; moiré domain-wall networks are not the central evidence in the base bilayer studies.	Moiré-specific device action is not directly established.	[14]

Table 2. *Cont.*

Material System	Polarization Origin	Characterizations	Switching / Domain-Wall Behavior	Functionalities and Issues	Refs.
Marginally twisted TMDs	Moiré reconstruction of MX/XM dipoles into polar domains; strain, pinning, screening, and domain-wall topology tune the response.	BSECCI/KPFM, operando TEM, STM, Raman, vector PFM, plasmonic imaging, and nano-photocurrent mapping resolve polar domains and dynamics.	Field-driven domain redistribution proceeds through domain-wall motion, partial-dislocation-network change, soliton-network evolution, and pinning-depinning.	Moiré FeFETs, remote band-structure control, graphene/twisted-WSe_2 transport response, and plasmonic or photocurrent readout. Deterministic control of domain-wall motion, pinning, and device uniformity remains unresolved.	[33–36,42,80]
WTe_2/WSe_2 heterostructures	Switchable WTe_2 polarization modulates the WTe_2/WSe_2 moiré potential through polarization-dependent charge transfer.	Transport versus filling and displacement field, PFM, nonlinear anomalous Hall response, and temperature-dependent resistance show switchable moiré potentials.	Vertical-field reversal changes interlayer charge transfer and moiré potential depth; domain-wall dynamics were not the main resolved process.	Nonvolatile control of moiré insulating states and nonlinear anomalous Hall response. Real-space domain-wall dynamics and microscopic switching pathways require further clarification.	[24]

5. Conclusions and Outlook

In summary, moiré ferroelectricity has advanced from phenomenological observation to a deeper mechanistic understanding. It represents a class of interfacial polar states. Its microscopic origin depends on stacking symmetry, local reconstruction, electronic screening and the specific material platform. Polarization switching in moiré systems may involve local stacking conversion, domain-wall migration, dislocation-network rearrangement, soliton-like reconstruction and pinning-depinning processes. Domain walls act as mobile structural units. They mediate local stacking conversion, accommodate elastic relaxation and define the kinetic pathway of polarization reversal. Topological polar textures further extend this mechanistic framework. Their identification should be supported by reconstructed polarization vector fields, in-plane polarization rotation, winding number or chirality, and structural correlation at domain walls, saddle-point regions or reconstructed interfaces. The emergence of polar meron-antimeron-like networks, vortex-like in-plane polarization and edge-related polar topology indicates that moiré ferroelectrics can host low-dimensional polar textures. These textures are closely tied to local stacking, strain gradients, domain-wall geometry and electromechanical coupling.

Despite these advances, several key challenges remain. The first challenge is operando characterization under realistic device conditions. Many moiré ferroelectric structures contain buried interfaces or complex multilayer stacks. Direct access to local polarization, stacking registry and strain distribution remains difficult. Recent moiré ferroelectric field-effect transistors based on twisted WSe_2 have shown trap-suppressed, low-voltage and nonvolatile operation. Capacitance-voltage spectroscopy and modeling further indicate sub-microsecond switching [81]. These results show the device potential of moiré ferroelectricity. Moreover, intrinsic ferroelectric switching must be distinguished from charge trapping, electrostatic screening, contact effects and mechanically induced artifacts. Prior PFM and KPFM studies have shown that local hysteresis and surface-potential contrast can be affected by non-ferroelectric electromechanical responses, tip-sample electrostatic forces, screening charges and adsorbates [82,83]. In 2D devices, charge trapping, water or oxygen adsorption and contact-related carrier redistribution can also produce or modify electrical hysteresis [84]. For van der Waals interfaces, probe force should also be considered because nanoprobe-induced mechanical force has been shown to drive interlayer sliding and move moiré polar domains in twisted hBN interfacial ferroelectrics [37]. Therefore, single-channel evidence such as PFM phase contrast, KPFM potential maps, transport hysteresis or optical contrast should be checked against controls on sweep rate, pulse width, waiting time, atmosphere, encapsulation, probe force and contact geometry. More reliable assignment should be based on agreement among structural reconstruction, electrostatic potential, polarization response and functional readout.

The second challenge is the limited ability to probe ultrafast and transient switching dynamics. Polarization reversal, photoinduced polarization responses, carrier-screening dynamics and transient evolution of topological polar textures may occur on time scales beyond conventional scanning-probe measurements. The field still lacks experimental techniques that can combine femtosecond temporal resolution, ångström-level spatial precision and meV-scale energy resolution in a single operando measurement. This limitation makes it difficult to resolve the elementary steps of interlayer sliding, domain-wall motion and transient lattice reconstruction during switching [4]. Ultrafast TEM, X-ray free-electron laser measurements, pump-probe optical spectroscopy, high-speed electrical readout and operando transport microscopy will therefore be needed to access atomic-scale spatial and femtosecond temporal switching dynamics. Recent sliding-ferroelectric memories have demonstrated ultrafast and high-endurance switching performance [81,85]. This indicates that interlayer sliding can support technologically attractive switching dynamics. The microscopic speed limit of moiré ferroelectric switching still requires direct dynamic verification.

The third challenge is local characterization under coupled external fields. Moiré ferroelectricity can interact with strain, magnetism, correlated electronic states, excitons, superconductivity, optical selection rules and nonlinear photoresponses. A complete mechanistic understanding requires local probes under combined electric, mechanical, optical, magnetic and thermal stimuli. Recent double-moiré experiments have reported signatures of a flexoelectric polar vortex superstructure together with electronic-correlation-modulated screening [55]. Such studies would clarify how polar domains reshape electronic bands, how screening modifies ferroelectric stability, how domain walls couple to low-dimensional electronic states, and how topological polar textures influence nonlinear optical or transport responses.

Looking forward, the development of moiré ferroelectrics will likely follow two connected directions. The first is mechanism-oriented. Continued advances in vector-resolved PFM, 4D-STEM, operando TEM, nano-SHG, KPFM, nano-photocurrent imaging and plasmonic sensing should make it possible to build a quantitative structure-polarization-dynamics map. Such a map would clarify how local stacking, strain gradients, saddle-point geometry, domain-wall topology and electrostatic screening jointly determine polar textures and switching pathways. In this direction, strain-gradient coupling and flexoelectric modulation deserve particular attention as design variables for polar-domain and polar-texture engineering.

The second direction is function-oriented. With progress in near-zero-twist engineering, hBN encapsulation, cleaner van der Waals assembly and scalable material preparation, moiré ferroelectricity is beginning to move toward room-temperature and device-relevant operation. Room-temperature ferroelectric responses have been demonstrated in selected van der Waals and moiré-related heterostructures. For example, monolayer graphene sandwiched between hBN exhibits robust room-temperature ferroelectricity [54]. However, room-temperature robustness has not yet been established as a universal property of all moiré ferroelectric platforms.

Recent device-oriented studies further indicate that moiré ferroelectricity can be directly integrated into electronic functionality. A twisted WSe_2 moiré FeFET showed trap-suppressed low-voltage operation, a stable nonvolatile memory window and capacitance-based evidence for sub-microsecond switching [14]. Strain-mediated nonvolatile polarization in twisted moiré superlattices further showed that stress engineering can reconstruct domain-wall configurations, overcome antiferroelectric or volatile switching tendencies and stabilize nonvolatile polarization, suggesting a route toward mechanically programmable low-power memory platforms [58]. In graphene coupled to twisted WSe_2 moiré ferroelectricity, the polar moiré potential was used to induce a near-room-temperature metal-insulator transition, illustrating how moiré ferroelectricity can act as a programmable functional substrate [80]. However, The success of these device concepts will depend on whether polarization switching can be made deterministic, fast, fatigue-resistant and spatially uniform across large areas. Beyond memory and transistor concepts, moiré ferroelectricity also provides a route for reconfigurable electronic and optoelectronic landscapes. Remote moiré ferroelectricity has been used to engineer band structures in adjacent 2D materials, suggesting that a polar moiré layer can serve as a programmable electrostatic template without being the active transport channel itself [34]. Ferroelectric moiré domains in twisted hBN can also modulate light emission from an adjacent semiconductor monolayer [40]. These studies expand the role of moiré ferroelectrics to reconfigurable functional substrates for electronic, excitonic and optoelectronic devices.

Author Contributions

Y.Y.: methodology, formal analysis, data curation, writing—original draft. J.L.: investigation, formal analysis, review. Y.R.: investigation, review & editing. All authors have read and agreed to the published version of the manuscript.

Funding

This research received no external funding.

Data Availability Statement

No data was used for the research described in the article.

Conflicts of Interest

The authors declare no conflict of interest. Yutong Ran is an employee of Grikin Advanced Materials Co., Ltd. The authors declare that this affiliation is the only potential conflicts of interest related to this work and that they did not influence the design, execution, analysis, interpretation, or presentation of the research.

Use of AI and AI-Assisted Technologies

During the preparation of this work, the authors used ChatGPT to polish the text and figures in the paper. After using this tool, the authors reviewed and edited the content as needed and take full responsibility for the content of the published article.

References

1. Wu, M. 100 years of ferroelectricity. *Nat. Rev. Phys.* **2021**, *3*, 726–726.
2. Wang, C.; You, L.; Cobden, D.; et al. Towards two-dimensional van der Waals ferroelectrics. *Nat. Mater.* **2023**, *22*, 542–552.
3. Yuan, S.; Luo, X.; Chan, H.L.; et al. Room-temperature ferroelectricity in $MoTe_2$ down to the atomic monolayer limit. *Nat. Commun.* **2019**, *10*, 1775.
4. Zhang, Q.; Fan, A.; Wang, Y.; et al. Emerging frontiers in two-dimensional sliding ferroelectrics. *npj 2D Mater. Appl.* **2025**, *9*, 76.
5. Gradauskaite, E.; Meier, Q.N.; Gray, N.; et al. Defeating depolarizing fields with artificial flux closure in ultrathin ferroelectrics. *Nat. Mater.* **2023**, *22*, 1492–1498.
6. Zhang, D.; Schoenherr, P.; Sharma, P.; et al. Ferroelectric order in van der Waals layered materials. *Nat. Rev. Mater.* **2022**, *8*, 25–40.
7. Vizner Stern, M.; Salleh Atri, S.; Ben Shalom, M. Sliding van der Waals polytypes. *Nat. Rev. Phys.* **2024**, *7*, 50–61.
8. Liu, F.; You, L.; Seyler, K.L.; et al. Room-temperature ferroelectricity in CuInP2S6 ultrathin flakes. *Nat. Commun.* **2016**, *7*, 12357.
9. Io, W.F.; Pang, S.-Y.; Wong, L.W.; et al. Direct observation of intrinsic room-temperature ferroelectricity in 2D layered $CuCrP_2S_6$. *Nat. Commun.* **2023**, *14*, 7304.
10. Zhao, C.; Dong, W.; Yang, Y.; et al. Intrinsic ferroelectric $CuVP_2S_6$ for potential applications in neuromorphic recognition and translation. *Nat. Commun.* **2025**, *16*, 6264.
11. Xiao, J.; Zhu, H.; Wang, Y.; et al. Intrinsic Two-Dimensional Ferroelectricity with Dipole Locking. *Phys. Rev. Lett.* **2018**, *120*, 227601.
12. Chang, K.; Liu, J.; Lin, H.; et al. Discovery of robust in-plane ferroelectricity in atomic-thick SnTe. *Science* **2016**, *353*, 274–278.
13. Vizner Stern, M.; Waschitz, Y.; Cao, W.; et al. Interfacial ferroelectricity by van der Waals sliding. *Science* **2021**, *372*, 1462–1466.
14. Wang, X.; Yasuda, K.; Zhang, Y.; et al. Interfacial ferroelectricity in rhombohedral-stacked bilayer transition metal dichalcogenides. *Nat. Nanotechnol.* **2022**, *17*, 367–371.
15. Wu, M.; Li, J. Sliding ferroelectricity in 2D van der Waals materials: Related physics and future opportunities. *Proc. Natl. Acad. Sci. USA* **2021**, *118*, e2115703118.
16. Yasuda, K.; Wang, X.; Watanabe, K.; et al. Stacking-engineered ferroelectricity in bilayer boron nitride. *Science* **2021**, *372*, 1458–1462.
17. Enaldiev, V.V.; Ferreira, F.; Magorrian, S.J.; et al. Piezoelectric networks and ferroelectric domains in twistronic superlattices in WS_2/MoS_2 and $WSe_2/MoSe_2$ bilayers. *2D Mater.* **2021**, *8*, 025030.
18. Enaldiev, V.V.; Ferreira, F.; Fal'ko, V.I. A Scalable Network Model for Electrically Tunable Ferroelectric Domain Structure in Twistronic Bilayers of Two-Dimensional Semiconductors. *Nano Lett.* **2022**, *22*, 1534–1540.
19. Zheng, Z.R.; Ma, Q.; Bi, Z.; et al. Unconventional ferroelectricity in moiré heterostructures. *Nature* **2020**, *588*, 71–76.
20. Nuckolls, K.P.; Yazdani, A. A microscopic perspective on moiré materials. *Nat. Rev. Mater.* **2024**, *9*, 460–480.

21. Ponomarenko, L.A.; Gorbachev, R.V.; Yu, G.L.; et al. Cloning of Dirac fermions in graphene superlattices. *Nature* **2013**, *497*, 594–597.
22. Hunt, B.; Sanchez-Yamagishi, J.D.; Young, A.F.; et al. Massive Dirac Fermions and Hofstadter Butterfly in a van der Waals Heterostructure. *Science* **2013**, *340*, 1427–1430.
23. Woods, C.R.; Ares, P.; Nevison-Andrews, H.; et al. Charge-polarized interfacial superlattices in marginally twisted hexagonal boron nitride. *Nat. Commun.* **2021**, *12*, 347.
24. Kang, K.; Zhao, W.; Zeng, Y.; et al. Switchable moiré potentials in ferroelectric WTe_2/WSe_2 superlattices. *Nat. Nanotechnol.* **2023**, *18*, 861–866.
25. Li, Y.; Wei, Y.; Guo, R.; et al. Unusual topological polar texture in moiré ferroelectrics. *Nat. Commun.* **2025**, *16*, 5451.
26. Bennett, D.; Remez, B. On electrically tunable stacking domains and ferroelectricity in moiré superlattices. *NPJ 2D Mater. Appl.* **2022**, *6*, 7.
27. Bennett, D. Theory of polar domains in moiré heterostructures. *Phys. Rev. B* **2022**, *105*, 235445.
28. Li, L.; Wu, M. Binary Compound Bilayer and Multilayer with Vertical Polarizations: Two-Dimensional Ferroelectrics, Multiferroics, and Nanogenerators. *ACS Nano* **2017**, *11*, 6382–6388.
29. Niu, R.; Li, Z.; Han, X.; et al. Ferroelectricity with concomitant Coulomb screening in van der Waals heterostructures. *Nat. Nanotechnol.* **2025**, *20*, 346–352.
30. Bennett, D.; Chaudhary, G.; Slager, R.-J.; et al. Polar meron-antimeron networks in strained and twisted bilayers. *Nat. Commun.* **2023**, *14*, 1629.
31. Xu, H.W.; Fan, W.C.; Zheng, J.D.; et al. Domain-Wall-Mediated Interfacial Ferroelectric Switching. *Nano Lett.* **2026**, *26*, 1043–1050.
32. Kim, D.S.; Dominguez, R.C.; Mayorga-Luna, R.; et al. Electrostatic moiré potential from twisted hexagonal boron nitride layers. *Nat. Mater.* **2024**, *23*, 65–70.
33. Zhang, S.; Liu, Y.; Sun, Z.; et al. Visualizing moiré ferroelectricity via plasmons and nano-photocurrent in graphene/twisted-WSe_2 structures. *Nat. Commun.* **2023**, *14*, 6200.
34. Ding, J.; Xiang, H.; Zhou, W.; et al. Engineering band structures of two-dimensional materials with remote moiré ferroelectricity. *Nat. Commun.* **2024**, *15*, 9087.
35. Ko, K.; Yuk, A.; Engelke, R.; et al. Operando electron microscopy investigation of polar domain dynamics in twisted van der Waals homobilayers. *Nat. Mater.* **2023**, *22*, 992–998.
36. Van Winkle, M.; Dowlatshahi, N.; Khaloo, N.; et al. Engineering interfacial polarization switching in van der Waals multilayers. *Nat. Nanotechnol.* **2024**, *19*, 751–757.
37. Guan, Z.; Wei, L.Q.; Fan, W.C.; et al. Mechanical force-induced interlayer sliding in interfacial ferroelectrics. *Nat. Commun.* **2025**, *16*, 986.
38. Pan, E.; Li, Z.; Yang, F.; et al. Observation and manipulation of two-dimensional topological polar texture confined in moiré interface. *Nat. Commun.* **2025**, *16*, 3026.
39. Wan, S.; Huang, H.; Liu, H.; et al. Intertwined Flexoelectricity and Stacking Ferroelectricity in Marginally Twisted hBN Moiré Superlattice. *Adv. Mater.* **2024**, *36*, 2410563.
40. Kim, D.S.; Xiao, C.; Dominguez, R.C.; et al. Moiré ferroelectricity modulates light emission from a semiconductor monolayer. *Sci. Adv.* **2025**, *11*, eadt7789.
41. Wei, L.; Zheng, Y.; Guan, Z.; et al. Multi-Terraced Stacking Engineering in Moiré Ferroelectric Superlattice. *Adv. Mater.* **2026**, *38*, e14265.
42. Singha, A.; Sett, S.; Watanabe, K.; et al. Moiré-Engineered Ferroelectric Transistors for Nearly Trap-Free, Low-Power, and Nonvolatile 2D Electronics. *ACS Nano* **2026**, *20*, 10544–10555.
43. Cohen, R.E. Origin of ferroelectricity in perovskite oxides. *Nature* **1992**, *358*, 136–138.
44. Deb, S.; Cao, W.; Raab, N.; et al. Cumulative polarization in conductive interfacial ferroelectrics. *Nature* **2022**, *612*, 465–469.
45. Wang, X.; Xu, C.; Aronson, S.; et al. Moiré band structure engineering using a twisted boron nitride substrate. *Nat. Commun.* **2025**, *16*, 178.
46. Xiao, Y.; Hu, W.; Li, K.; et al. Deep Moiré Potential and Absence of Layer Polarization in Twisted Trilayer WS_2. *Nano Lett.* **2025**, *25*, 6935–6941.
47. Shi, C.; Mao, N.; Zhang, K.; et al. Domain-dependent strain and stacking in two-dimensional van der Waals ferroelectrics. *Nat. Commun.* **2023**, *14*, 7168.
48. Han, K.; Cho, M.; Kim, T.; et al. Highly Tunable Moiré Superlattice Potentials in Twisted Hexagonal Boron Nitrides. *Adv. Sci.* **2025**, *12*, 2408034.
49. Guo, Z.-H.; Yan, C.; He, J.-Q.; et al. Manipulating Superlattice Potentials and Quantum Confinement in Graphene via Moiré Ferroelectricity. *Nano Lett.* **2025**, *25*, 11543–11548.

50. Zhang, S.; Fonseca, J.; Bennett, D.; et al. Plasmonic Polarization Sensing of Electrostatic Superlattice Potentials. *Phys. Rev. X* **2025**, *15*, 011019.
51. Cho, M.; Datta, B.; Han, K.; et al. Moiré Exciton Polaron Engineering via twisted hBN. *Nano Lett.* **2025**, *25*, 1381–1388.
52. Gu, L.; Zhang, L.; Felsenfeld, S.; et al. Quantum Confining Excitons with an Electrostatic Moiré Superlattice. *Phys. Rev. Lett.* **2025**, *135*, 026901.
53. Zhang, L.; Ding, J.; Xiang, H.; et al. Electronic ferroelectricity in monolayer graphene moiré superlattices. *Nat. Commun.* **2024**, *15*, 10905.
54. Lin, F.; Xuan, X.; Cao, Z.; et al. Room temperature ferroelectricity in monolayer graphene sandwiched between hexagonal boron nitride. *Nat. Commun.* **2025**, *16*, 1189.
55. Li, S.; Wang, Z.; Han, Y.; et al. Signatures of Flexoelectric Polar Vortex Superstructure and Electronic-Correlation-Modulated Screening in a Double-Moiré System. *Nano Lett.* **2026**, *26*, 5102–5111.
56. Hong, S.C.; Baek, J.-H.; Chang, Y.; et al. Overcoming the Lattice Mismatch Barrier for Atomic Reconstruction in $MoSe_2/MoS_2$ Heterobilayers. *ACS Nano* **2025**, *19*, 41233–41243.
57. Liu, H.; Lai, Q.; Fu, J.; et al. Reversible flexoelectric domain engineering at the nanoscale in van der Waals ferroelectrics. *Nat. Commun.* **2024**, *15*, 4556.
58. Fan, W.; Wei, L.; Tong, W.; et al. Strain-Mediated Non-Volatile Polarization in Twisted Moiré Superlattices. *Adv. Funct. Mater.* **2026**, *36*, e74888.
59. Wu, X.; Duan, W.; Li, J. Polarization Textures in Moiré Patterns of van der Waals Homo- and Heterostructures via Sliding Ferroelectrics. *Nano Lett.* **2025**, *25*, 12653–12659.
60. Zheng, J.; Yao, C.; Zhou, S.; et al. Machine Learning Exploration of Topological Polarization Pattern in Hexagonal Boron Nitride Moiré Superlattice. *Adv. Funct. Mater.* **2025**, *35*, 2503011.
61. Li, Y.; Ding, L.; Li, Z.; et al. Topological Polar Networks in Twisted Rhombohedral-Stacked Bilayer WSe_2 Moiré Superlattices. *Nano Lett.* **2024**, *24*, 13349–13355.
62. Fan, W.-C.; Guan, Z.; Wei, L.-Q.; et al. Edge polarization topology integrated with sliding ferroelectricity in Moiré system. *Nat. Commun.* **2025**, *16*, 3557.
63. Guan, Z.; Fan, W.C.; Wei, L.Q.; et al. Phase Transition of Moiré Edges in Interfacial Ferroelectrics. *ACS Nano* **2025**, *19*, 39220–39227.
64. Hassan, Y.; Singh, B.; Joe, M.; et al. Twist-Controlled Ferroelectricity and Emergent Multiferroicity in WSe_2 Bilayers. *Adv. Mater.* **2024**, *36*, 2406290.
65. Shin, Y.-H.; Grinberg, I.; Chen, I.-W.; et al. Nucleation and growth mechanism of ferroelectric domain-wall motion. *Nature* **2007**, *449*, 881–884.
66. Catalan, G.; Seidel, J.; Ramesh, R.; et al. Domain wall nanoelectronics. *Rev. Mod. Phys.* **2012**, *84*, 119–156.
67. Yang, D.; Liang, J.; Wu, J.; et al. Non-volatile electrical polarization switching via domain wall release in 3R-MoS_2 bilayer. *Nat. Commun.* **2024**, *15*, 1389.
68. Molino, L.; Aggarwal, L.; Enaldiev, V.; et al. Ferroelectric Switching at Symmetry-Broken Interfaces by Local Control of Dislocations Networks. *Adv. Mater.* **2023**, *35*, 2207816.
69. Li, Y. Soliton Disentangling and Ferroelectric Hysteresis in Bilayer MoS_2 Nanostructures with Reconstructed Moiré Superlattices. *ACS Appl. Nano Mater.* **2022**, *5*, 17461–17467.
70. Chen, J.; Ke, C.; Bian, R.; et al. Deterministic 1D Domain Wall Motion with Nucleation-Free Nature in Sliding Ferroelectric Switching. *Phys. Rev. X* **2026**, *16*, 011066.
71. Ke, C.; Liu, F.; Liu, S. Superlubric Motion of Wavelike Domain Walls in Sliding Ferroelectrics. *Phys. Rev. Lett.* **2025**, *135*, 046201.
72. Chiodini, S.; Venturi, G.; Kerfoot, J.; et al. Electromechanical Response of Saddle Points in Twisted hBN Moiré Superlattices. *ACS Nano* **2025**, *19*, 16297–16306.
73. Sangers, J.J.M.; Brokkelkamp, A.; Conesa-Boj, S. Strain-Induced Moiré Polarization Vortices in Twisted-Multilayer WSe_2. *Small* **2025**, *21*, 2503363.
74. Yao, K.; Zhang, S.; Yanev, E.; et al. Nanoscale Optical Imaging of 2D Semiconductor Stacking Orders by Exciton-Enhanced Second Harmonic Generation. *Adv. Opt. Mater.* **2022**, *10*, 2200085.
75. Rosas-Hernandez, L.E.; Cabellos, J.L.; Huamán, A.; et al. Insulating moiré homobilayers lack a threefold symmetric second-harmonic generation. *Phys. Rev. Mater.* **2024**, *8*, 116203.
76. Katsura, H.; Nagaosa, N.; Balatsky, A.V. Spin Current and Magnetoelectric Effect in Noncollinear Magnets. *Phys. Rev. Lett.* **2005**, *95*, 057205.
77. Ramesh, R.; Spaldin, N.A. Multiferroics: progress and prospects in thin films. *Nat. Mater.* **2007**, *6*, 21–29.
78. Zhu, H.; Yu, H.; Zhu, W.; et al. Moiré-Induced Magnetoelectricity in Twisted Bilayer NiI_2. *Phys. Rev. Lett.* **2025**, *135*, 196701.

79. Antão, T.V.C.; Lado, J.L.; Fumega, A.O. Electric Field Control of Moiré Skyrmion Phases in Twisted Multiferroic NiI_2 Bilayers. *Nano Lett.* **2024**, *24*, 15767–15773.
80. Singh, B.; Hassan, Y.; Ali, N.; et al. Quantum Phase Transitions in Graphene Coupled to a Twisted WSe_2 Moiré Ferroelectricity. *Adv. Mater.* **2026**, *38*, e14744.
81. Bian, R.; He, R.; Pan, E.; et al. Developing fatigue-resistant ferroelectrics using interlayer sliding switching. *Science* **2024**, *385*, 57–62.
82. Seol, D.; Park, S.; Varenyk, O.V.; et al. Determination of ferroelectric contributions to electromechanical response by frequency dependent piezoresponse force microscopy. *Sci. Rep.* **2016**, *6*, 30579.
83. Segura, J.J.; Domingo, N.; Fraxedas, J.; et al. Surface screening of written ferroelectric domains in ambient conditions. *J. Appl. Phys.* **2013**, *113*, 187213.
84. Late, D.J.; Liu, B.; Matte, H.S.S.R.; et al. Hysteresis in Single-Layer MoS_2 Field Effect Transistors. *ACS Nano* **2012**, *6*, 5635–5641.
85. Yasuda, K.; Zalys-Geller, E.; Wang, X.; et al. Ultrafast high-endurance memory based on sliding ferroelectrics. *Science* **2024**, *385*, 53–56.